Intelektual Journal of Energy Harvesting and Storage
Vol. 1, No. 2, 2023, pp. 68~81
ISSN: 2963-6272, DOI: 10.11591/ehs.v1i2.pp68-81

Improvement of doubly fed induction generator wind energy conversion system using robust backstepping non linear control

Hasnaa Jenkal[1], Mouna Lamnadi[1], Sara Mensou[2], Badre Bossoufi[3], Abdelkader Boulezhar[1]
[1]Laboratory of Renewable Energy and Dynamic of Systems, Faculty of Sciences Ain-Chock, University Hassan II, Casablanca, Morocco
[2]Electrical Engineering Department of ENSET, Mohammed V University, Rabat, Morocco
[3]LIMAS Laboratory Faculty of Sciences, Sidi Mohamed Ben Abdellah University, Fez, Morocco

Article Info

Article history:

Received May 29, 2023
Revised Oct 8, 2023
Accepted Nov 12, 2023

Keywords:

Backstepping
Doubly fed induction generator
Maximum power point tracker
Control
Modelling
Wind turbine

ABSTRACT

In this paper, we present a robust control of the doubly fed induction generator (DFIG) using in the wind energy conversion system (WECS). We started by using the maximum power point tracker (MPPT) method to extract the maximum power in the WECS, then modeling DFIG and applied the Backstepping method in order to control the reactive power, and electromagnetic torque. The details of the control strategy and the simulation of all the system components were performed using MATLAB/Simulink software. The results presented in this paper are used to evaluate the efficiency of the proposed control strategy.

Corresponding Author:

Hasnaa Jenkal
Laboratory of Renewable Energy and Dynamic of Systems, Faculty of Sciences Ain-Chock,
University Hassan II
Casablanca Morocco
Email: jenkal.hasnaa@gmail.com or hasnaa.jenkal-etu@etu.univh2c.ma

1. INTRODUCTION

Recently, three-bladed horizontal axis wind turbines based on a doubly fed induction generator (DFIG) are the most exploited in the wind power system industry, the structure of these systems is based on the installation of two electronic power converters, a converter of generator-side power and a grid-side power converter, these are used to allow the DFIG to operate at variable speeds. The modeling of any system is an important and necessary phase for the study and control of its operation [1], [2] in this work we will approach the modeling of the elements of the wind system, necessary for the transition from a kinetic movement of the wind to electrical energy. All the constituent elements of the wind power chain have been developed and modeled to simulate them in the Simulink software, in order to visualize the temporal evolution of its various representative variables, to study the behavior of the wind power system, and to be able to make a determination control laws and control techniques that will be adapted to the system studied.

There is the profitability index (PI) method for it is reliability and its simplicity of implementation in different control boards, so it keeps its performance [3] for the cases of linear systems with constant parameters, but for nonlinear systems which require a certain precision and stability, it remains insufficient and suffers from instability during a large fluctuation of the system parameters. For these reasons, in our thesis work, we have used a second command as a solution to the problems. Relating to the first, it is the nonlinear Backstepping command which is one of the commands that have proven their stability, performance and robustness against disturbances. We will discuss our first research activity devoted to the

study of turbine control by the maximum power point tracker (MPPT) method to recover the maximum power produced and optimize energy efficiency. During the second part, we will first talk about the theoretical tools necessary to present control algorithms such as the notions of stability in the sense of Lyapunov and the Backstepping algorithm. Then, we will detail the mathematical development which led to the synthesis of the laws of the Backstepping command, we will finish by representing the results of simulation for the possibilities of fluctuations of internal parameters of the generator.

2. WIND TURBINE

Currently, the variable-speed wind system based on a double-fed asynchronous generator (DFIG) is the most widely used. Its main advantage is to have its three-phase static converters sized for part of the nominal power of the DFIG, which generates a significant economic benefit compared to other solutions used (for example: synchronous generator with permanent magnets) [4], [5]. The wind turbine drives via a speed multiplier, where it is connected directly to the electrical network by the stator and by the rotor through two three-phase static converters controlled in pulse width modulation (PWM); one on the rotor side of DFID called rotor side converter (RSC) and the other on the power grid side called grid side converter. In this part, we model the wind conversion chain, and we present the DFIG model in Park model (d, q).

2.1. Wind turbine modelling

The wind power corresponding to an undisturbed wind is expressed in [6]:

$$P_v = \frac{\rho s v^3}{2} \quad (1)$$

The aerodynamic torque appearing at the turbine is a function of this power:

$$P_{aero} = C_p(\lambda, \beta) * P_v = \frac{1}{2} * \pi * R^2 * v^3 * C_p(\lambda, \beta) \quad (2)$$

The evolution of the power coefficient Cp depends on the aerodynamic characteristics of the wind turbine as well as the operating conditions [3]. For a fixed pitch angle β, the power coefficient Cp can be expressed as a function of the speed ratio λ. For a variable pitch angle, the power coefficient can be expressed as a function of λ and β, which is given as:

$$\lambda = \frac{\Omega_t * R}{v} \quad (3)$$

where, P_v, is the captured power of the wind turbine, ρ , is the air density, v, is the wind speed, **Ω**, is the angular speed (m/s) and R is the length of the blade (m)

Albert Betz calculated the maximum of C_p as following [7]:

$$C_{pmax}(\lambda, \beta) = \frac{16}{27} = 0.5926 \quad (4)$$

The expression of this power coefficient has been approached for this type of turbine, by (5) [8]:

$$C_p(\lambda, \beta) = \left(0.5 - 0.0167 * (\beta - 2)\right) * \sin\left(\frac{\pi * (\lambda + 0.1)}{18.5 - 0.3 * (\beta - 2)}\right) - 0.00184 * (\beta - 2) * (\lambda - 3) \quad (5)$$

here it can be clearly seen that for a given pitch angle, there exists a nominal tip speed ratio (λnom), that maximizes C_p (λ, β) as shown in Figure 1 and hence maximizes the power output of the turbine for a given wind speed. Therefore, it is highly desirable to be able to change the speed of the turbine as the wind speed changes, such that the turbine maintains the nominal tip speed ratio.

The aerodynamic torque is given as:

$$C_t = \frac{P_{aero}}{\Omega_t} = C_p(\lambda, \beta) * \frac{\pi * R^2 * v^3}{2\Omega_t} \quad (6)$$

The gearbox is utilized as a connection, to adjust the speed of the turbine to that of the generator. The energy losses [9], versatility and grating in the gearbox are disregarded so:

$$\Omega_{mec} = \Omega_t * G$$

$C_t = C_g * G$ (6)

The fundamental equation of dynamics is giving as

$$T_{mec} = J * \frac{d\Omega_{mec}}{dt} = T_g - T_{em} - f * \Omega_{mec} \quad (7)$$

$$T_{em} = \frac{1}{2} * \pi * \rho * R^5 * \frac{C_{pmax}}{\lambda_{opti}^3} \quad (8)$$

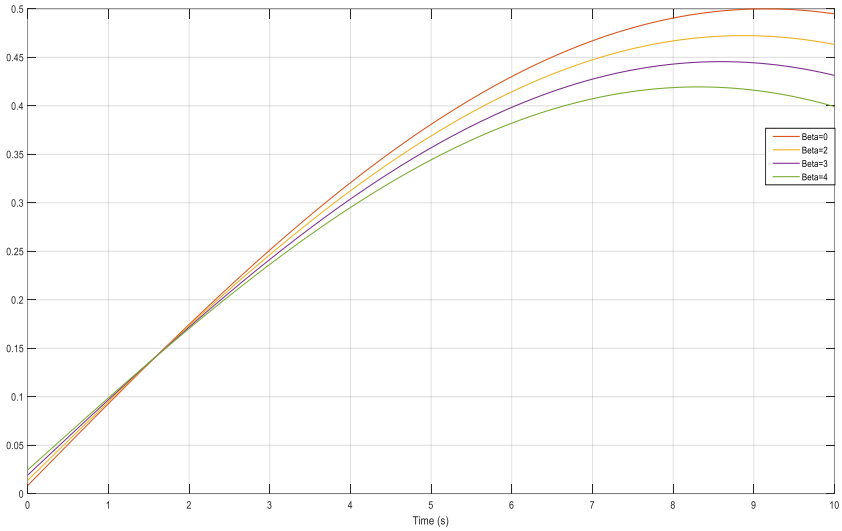

Figure 1. Aerodynamic power coefficient $C_p(\lambda, \beta)$

2.2. MPPT control

The variable-speed wind turbine increases the energy efficiency and improves the quality of the energy produced compared to that operating at a fixed speed [6], [10]. To maximize the power captured, the maximum power extraction technique (MPPT) is applied. Figure 2 shows the principle of MPPT control of wind turbine, the ratio of the speed of wind λ must be maintained at its optimum value $\lambda=\lambda_{opti}$ on a certain wind speed range. Tus, the power coefficient would be maintained at its maximum value. The control objective is to optimize the capture wind energy by tacking the optimal torque.

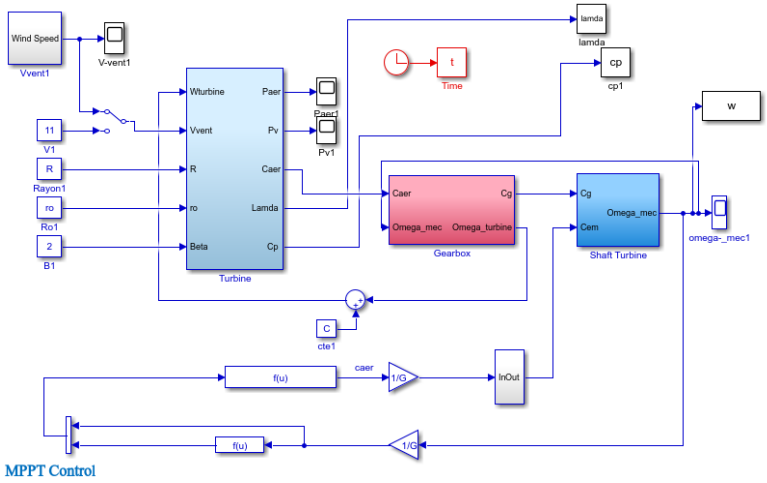

Figure 2. Diagram of the wind turbine and MPPT control

3. DOUBLE FED INDUCTION GENERATOR MODELLING

The modelling of the DFIG is similar to the induction generator as shown Figure 3. The DFIG dynamic equation of a three-phase DFIG can be written in a synchronously rotation direct-quadrature (d-q) reference frame as [1], [11]. The electrical by (9) and (10):

$$\begin{cases} V_{sd} = R_s I_{sd} + \frac{d\Phi_{sd}}{dt} - \omega_s \Phi_{sq} \\ V_{sq} = R_s I_{sq} + \frac{d\Phi_{sq}}{dt} + \omega_s \Phi_{sd} \\ V_{rd} = R_r I_{rd} + \frac{d\Phi_{rd}}{dt} - \omega_r \Phi_{rq} \\ V_{rq} = R_r I_{rq} + \frac{d\Phi_{rq}}{dt} - \omega_r \Phi_{rd} \end{cases} \quad (9)$$

$$\begin{cases} I_{sd} = \frac{1}{\sigma L_S} \Phi_{sd} - \frac{M}{\sigma L_r L_S} \Phi_{rd} \\ I_{sq} = \frac{1}{\sigma L_S} \Phi_{sd} - \frac{M}{\sigma L_r L_S} \Phi_{rd} \\ I_{rd} = -\frac{M}{\sigma L_S L_r} \Phi_{sd} + \frac{1}{\sigma L_r} \Phi_{rd} \\ I_{rq} = -\frac{M}{\sigma L_S L_r} \Phi_{sq} + \frac{1}{\sigma L_r} \Phi_{rq} \end{cases} \quad (10)$$

The magnetic by (11):

$$\begin{aligned} \Phi_{sd} &= L_s i_{sd} + L_m i_{rd} \\ \Phi_{sq} &= L_s i_{sq} + L_m i_{rq} \\ \Phi_{rd} &= L_r i_{rd} + L_m i_{sd} \\ \Phi_{rq} &= L_r i_{rq} + L_m i_{sq} \end{aligned} \quad (11)$$

The stator/rotor active and reactive power are giving as (12):

$$\begin{aligned} P_s &= V_{sd} i_{sd} + V_{sq} i_{sq} \\ Q_s &= V_{sq} i_{sd} - V_{sd} i_{sq} \\ P_r &= V_{rd} i_{rd} + V_{rq} i_{rq} \\ Q_r &= V_{rq} i_{rd} - V_{rd} i_{rq} \end{aligned} \quad (12)$$

The electromagnetic torque is expressed as (13):

$$T_{em} = p * (I_{sq} * \Phi_{sd} + I_{sd} * \Phi_{sq}) \quad (13)$$

Where, V_{sd}, V_{sq} is stator voltages in d-q axis reference frame, V_{rd}, V_{rq} is rotor voltages in d-q axis reference frame, i_{sd}, i_{sq} is stator currents in d-q axis reference frame, i_{rd}, i_{rq} is rotor currents in d-q axis reference frame, L_s, L_r, m is self and mutual inductances of stator and rotor windings, respectively, R_s, R_r is the stator and rotor resistance, Φ_{sd}, Φ_{sq} is stator flux linkages in d-q axis reference, Φ_{rd}, Φ_{rq} is stator flux linkages in d-q axis reference, and p is number of machine pole pairs.

Power control strategy: to simplify the study of the power control strategy, we use a vector control of DFIG based on stator field oriented (SFO), by setting the stator field matched up with d-axis.
Choice of reference:

$$\begin{aligned} V_{sd} &= \frac{d\Phi_{sd}}{dt} \\ V_{sq} &= \omega_s \Phi_s \end{aligned} \quad (14)$$

With the hypothesis of constant stator flux, one obtains:

$$\begin{aligned} V_{sd} &= 0 \\ V_{sq} &= \Phi_s * \omega_s \end{aligned} \quad (15)$$

For the control of the generator, expressions are established showing the relationship between the currents and the rotor tensions that will be applied to it:

$$V_{rd}=R_r * i_{rd}+(L_r - \frac{Lm^2}{L_s}) * \frac{di_{rd}}{dt} -\left(L_r - \frac{L_m^2}{L_s} \right) * \omega_r * i_{rq}$$
$$V_{rq}=R_r * i_{rq}+(L_r - \frac{Lm^2}{L_s}) * \frac{di_{rq}}{dt} -\left(L_r - \frac{L_m^2}{L_s} \right) * \omega_r * i_{rd} + \omega_r * \frac{Lm}{L_s} * \Phi_s \quad (16)$$

The statoric power is controlled by the rotor voltages, it is an independent control of active and reactive powers on the d-q reference frame, as shown in Figure 4, and we can write as (17). The diagram blo:

$$P_s = V_{sd} i_{sd} + V_{sq} i_{sq} = - V_s * (\frac{Lm}{L_s}) * i_{rq}$$
$$Q_s = V_{sq} i_{sd} - V_{sd} i_{sq} = V_s * \frac{\Phi_s}{L_s} - V_s * (\frac{Lm}{L_s}) * i_{rd} \quad (17)$$

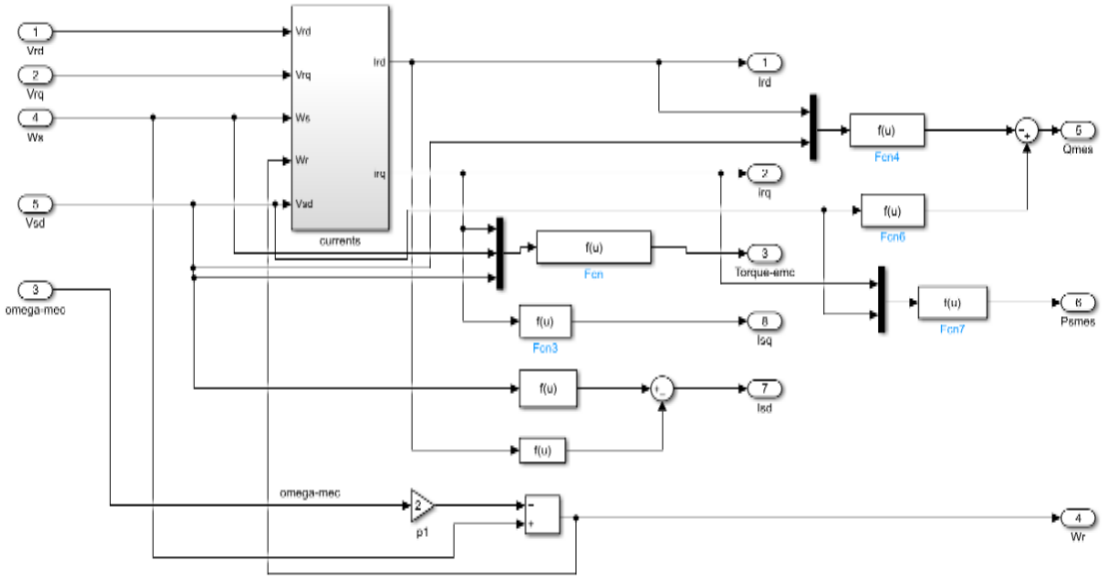

Figure 3. Diagram block of DFIG

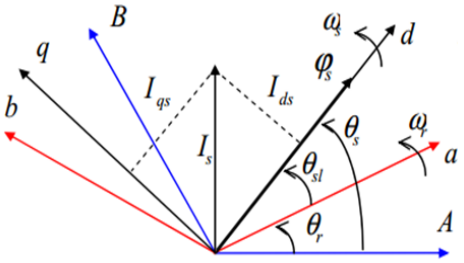

Figure 4. abc to dq

4. BACKSTEPPING CONTROL TECHNIQUE

The technique of backstepping consists in making a nonlinear complex dynamic system equivalent to simple subsystems of order 1, in cascade and stable in the sense of Lyapunov, which gives them a good quality of robustness [12]. The backstepping command is a multi-step method, in each step a virtual command is generated and intermediate command laws are developed to ensure the convergence of the system towards a stable equilibrium state, this can be achieved from the functions of Lyapunov who ensure step by step the stabilization of each synthesis step.

To facilitate the application of this technique it is necessary to make the model of the system in strict parametric form, that is to say that the derivative of each variable of the state vector must be a function of the preceding variables and which depends thereafter on the next variable.

The system should take the following form:

$$\begin{aligned}\dot{x}_1 &= f_1(x_1) + g_1(x_1)x_2 \\ \dot{x}_2 &= f_2(x_1, x_2) + g_2(x_1, x_2)x_3 \\ \dot{x}_3 &= f_3(x_1, x_2, x_3) + g_3(x_1, x_2, x_3)x_4 \\ \dot{x}_n &= f_n(x_1, x_2, x_3 \dots x_n) + g_n(x_1, x_2, x_3 \dots x_n)u\end{aligned} \quad (18)$$

With, x(t) represents the n state variables and u represents the control variable.

To illustrate the principle of backstepping, we consider a time-varying, dynamic and non-linear system of order 2, which is given by:

$$\begin{aligned}\dot{x}_1 &= f_1(x_1) + g_1(x_1)x_2 \\ \dot{x}_2 &= f_2(x_1, x_2) + g_2(x_1, x_2)x_2 \\ y &= x_1\end{aligned} \quad (19)$$

The purpose of the method is to control the quantity x_1, and to forward the output y=x1 of the system to a reference noted yref(t), the design of the command will be developed in two stages according to the order number of the system [13].

First step:

– We choose the first equation, where the variable x_2 is estimated as a virtual control variable:

$$\begin{aligned}\dot{x}_1 &= f_1(x_1) + g_1(x_1)x_2 \\ y &= y_{ref} = (x_1)_d\end{aligned} \quad (20)$$

– We then define the error variable e_1

$$e_1 = (x_1)_d - x_1 \quad (21)$$

– We calculate its derivative:

$$\dot{e_1} = \dot{(x_1)}_d - \dot{x_1} \quad (22)$$

– Consider the Lyapunov control function obtained by the (23):

$$V_1(e_1) = \frac{1}{2}e_1^2 \quad (23)$$

– We then calculate its total derivative:

$$\dot{V_1} = e_1\dot{e_1} = e_1[\dot{(x_1)}_d - \dot{x_1}] = e_1\left[\dot{(x_1)}_d - \dot{x_1}\right] = e_1\left[\dot{(x_1)}_d - f_1(x_1)\right) - g_1(x_1)x_2] \quad (24)$$

With:

$$\dot{V_1}(e_1) = -k_1e_1^2$$

– To guarantee the stability of the control, the derivative of the error must be negative:

$$\dot{(x_1)}_d - f_1(x_1) - g_1(x_1)x_2 < 0 \; and \; k_1 > 0 \quad (25)$$

– Which will allow us to calculate the virtual control variable x_2:

$$(x_2)_d = \frac{k_1e_1 - f_1(x_1) + \dot{(x_1)}_d}{g_1(x_1)} \quad (26)$$

Second step:

– We now choose the overall system:

$$\dot{x}_1 = f_1(x_1) + g_1(x_1)x_2$$
$$\dot{x}_2 = f_2(x_1, x_2) + g_2(x_1, x_2)u \quad (27)$$

Now the real command u, will appear in this step, we must follow the same steps to calculate the real control variable u, but this time with a new Lyapunov function, which is of the form [14]:

$$V(e_1, e_2) = \frac{1}{2}e_1^2 + \frac{1}{2}e_2^2 \quad (28)$$

– The total derivative of Lyapunov's function:

$$\dot{V_1}(e_1e_2) = e_1\dot{e_1} + e_2\dot{e_2} = -k_1e_1^2 - k_2e_2^2 \quad (29)$$

With:

$$\dot{V_1}(e_1e_2) < 0 \; and \; k_2 > 0$$

– We can deduce the true control variable u:

$$u = \frac{k_2e_2 - f_2(x_1,x_2) + \dot{(x_2)_d}}{g_2(x_1,x_2)} \quad (30)$$

4.1. Stator reactive power and torque control

Torque and reactive power errors:

$$\begin{cases} e_1 = T_{em}^* - T_{em} \\ e_2 = Q_s^* - Q_s \end{cases} \quad (31)$$

The derivative of torque and reactive power errors:

$$\begin{cases} \dot{e_1} = \dot{T_{em}^*} - \dot{T_{em}} \\ \dot{e_2} = \dot{Q_s^*} - \dot{Q_s} \end{cases} \quad (32)$$

$$\begin{cases} \dot{e_1} = \dot{T_{em}^*} + \frac{pL_mV_s}{L_s\omega_s}\left(-BI_{rq} - \omega_rI_{rd} - C\varphi_s\omega_r + AV_{rq}\right) \\ \dot{e_2} = \dot{Q_s^*} + \frac{V_sL_m}{L_s}\left(-BI_{rd} + \omega_rI_{rq} + AV_{rd}\right) \end{cases} \quad (33)$$

We use the "Lyapunov" function, to ensure the stability of the control [14]:

$$v_1 = \frac{1}{2}{e_1}^2 + \frac{1}{2}{e_2}^2 \quad (34)$$

The derivative of Lyapunov's candidate function:

$$\dot{v_1} = e_1\left(\dot{T_{em}^*} + \frac{pL_mV_s}{L_s\omega_s}(-BI_{rq} - \omega_rI_{rd} - C\varphi_s\omega_r + AV_{rq})\right) + e_2\left(\dot{Q_s^*} + \frac{V_sL_m}{L_s}(-BI_{rd} + \omega_rI_{rq} + AV_{rd})\right) \quad (35)$$

To guarantee the stability and good control of the system, the derivative of the Lyapunov function must be negative and the gains k_1, k_2 positive [15]:

$$\dot{V_1}(e_1) = -k_1e_1^2 - k_2e_2^2 < 0 \quad (36)$$

Virtual rotor current control variables:

$$\begin{cases} I_{rq} *= \left(\frac{L_s\omega_s}{BpL_mV_s}(\dot{T_{em}^*} + k_1e_1) + \frac{1}{R_r}(V_{rq} - \frac{\omega_r}{A}I_{rd} - \frac{C}{A}\varphi_s\omega_r)\right) \\ I_{rd} *= \left(\frac{L_s}{BL_mV_s}(\dot{Q_s^*} + k_2e_2) + \frac{1}{R_r}(V_{rd} + \frac{\omega_r}{A}I_{rq})\right) \end{cases} \quad (37)$$

4.2. Control of rotor currents

Rotor current errors:

$$\begin{cases} e_3 = I_{rq}^* - I_{rq} \\ e_4 = I_{rd}^* - I_{rd} \end{cases} \quad (38)$$

The derivative of the Errors of the currents:

$$\begin{cases} \dot{e_3} = \dot{I_{rq}^*} - \dot{I_{rq}} \\ \dot{e_4} = \dot{I_{rd}^*} - \dot{I_{rd}} \end{cases} \quad (39)$$

We replace the derivative of the currents by their expressions:

$$\begin{cases} \dot{e_3} = \dot{I_{rq}^*} - (\alpha V_{rq} - \delta I_{rq} - \omega_r I_{rd} - \gamma\varphi_s\omega_r) \\ \dot{e_4} = \dot{I_{rd}^*} - (\alpha V_{rd} - \delta I_{rd} + \omega_r I_{rq}) \end{cases} \quad (40)$$

We use the "Lyapunov" function, to ensure the stability of the control:

$$V_2 = \frac{1}{2}{e_1}^2 + \frac{1}{2}{e_2}^2 + \frac{1}{2}{e_3}^2 + \frac{1}{2}{e_4}^2 \quad (41)$$

The derivative of Lyapunov's candidate function:

$$\begin{aligned} &\dot{V_2} = e_1\dot{e_1} + e_2\dot{e_2} + e_3\dot{e_3} + e_4\dot{e_4} \\ &\dot{V_2} = e_1\dot{e_1} + e_2\dot{e_2} + e_3\left(\dot{I_{rq}^*} - (AV_{rq} - BI_{rq} - \omega_r I_{rd} - C\varphi_s\omega_r)\right) + e_4\left(\dot{I_{rd}^*} - (AV_{rd} - BI_{rd} + \omega_r I_{rq})\right) \end{aligned} \quad (42)$$

With k_1, k_2, k_3 and k_4 as positive constants

$$\begin{aligned} &\dot{V_2} = -k_1{e_1}^2 - k_2{e_2}^2 - k_3{e_3}^2 - k_4{e_4}^2 \leq 0 \\ &\begin{cases} V_{rq}^* = \frac{1}{\alpha}\left(\frac{L_s\omega_s}{\delta pL_mV_s}(\dot{T_{em}^*} + k_1e_1) + \frac{1}{R_r}(V_{rq} - \frac{\omega_r}{\alpha}I_{rd} - \frac{\gamma\varphi_s\omega_r}{\alpha}) + k_3e_3 + A\right) \\ V_{rd}^* = \frac{1}{\alpha}\left(\frac{L_s}{\delta L_mV_s}(\dot{Q_s^*} + k_2e_2) + \frac{1}{R_r}(V_{rd} + \frac{\omega_r}{\alpha}I_{rq}) + k_4e_4 + B\right) \end{cases} \end{aligned} \quad (43)$$

5. SIMULATIONS AND RESULTS

5.1. Backstepping control DFIG results

We apply a random wind profile, which changes between 8.5 and 13 m/s. It shows clearly in Figure 6. For the Figures 7-9 the control has as input the torque error, the reactive stator power error, the rotor current error Ir in d-q. The output makes it possible to evaluate the reference vector to drive the torque, the reactive stator power and the rotor currents Ir according to d-q towards their reference values during a period of time, in this simulation results we observe that the errors converge towards zero, which means that our method control is robust.

The reactive stator power Figure 10 has a zero value, to ensure a unity factor on the network side, we also notice that the electromagnetic torque Figure 11 follows its reference setpoint, which is extracted from the MPPT control, in addition the electromagnetic torque varies in the same way as the wind speed to make our machine run at a speed optimal which allows to obtain the maximum power, and in Figure 12 we can see that the current I_{rq} follows its reference.

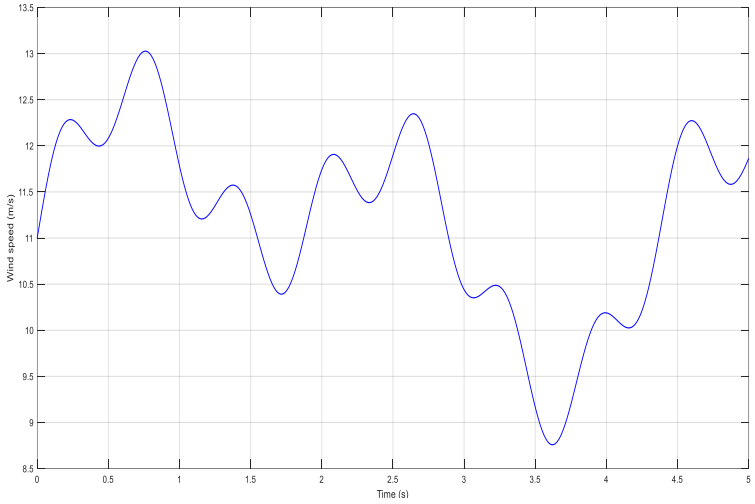

Figure 6. Wind speed (m/s)

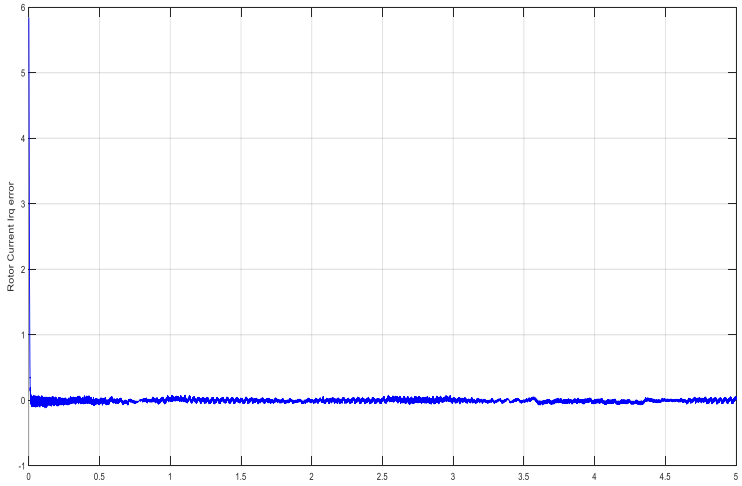

Figure 7. Rotor current I_{rq} error

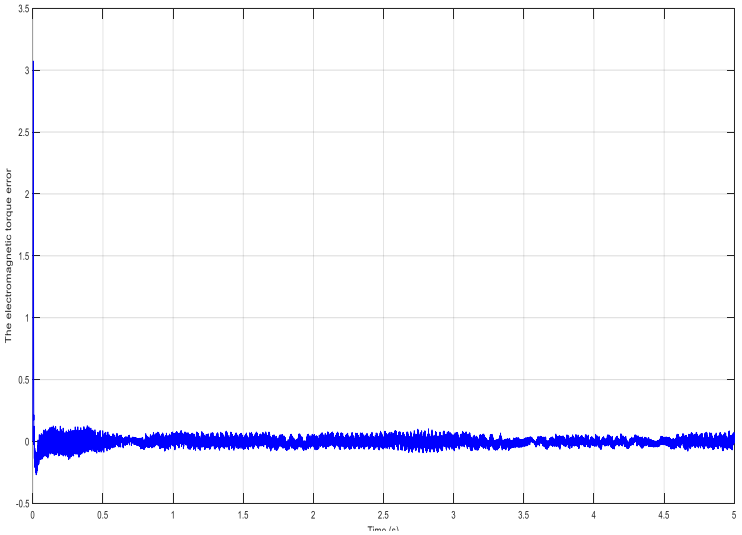

Figure 8. The electromagnetic torque error

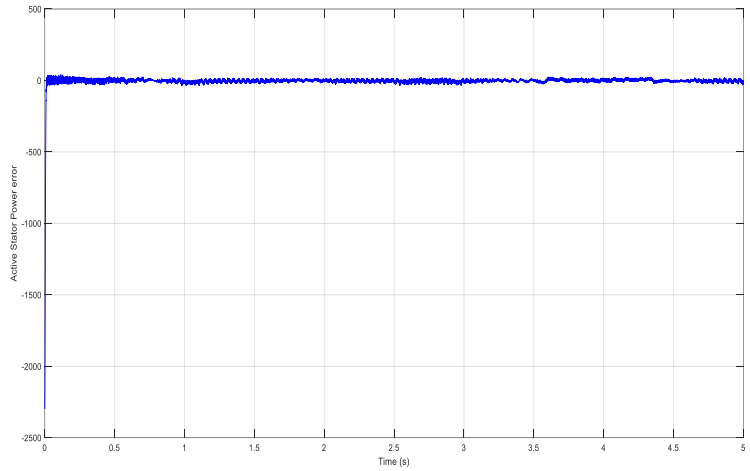

Figure 9. Reactive stator power error

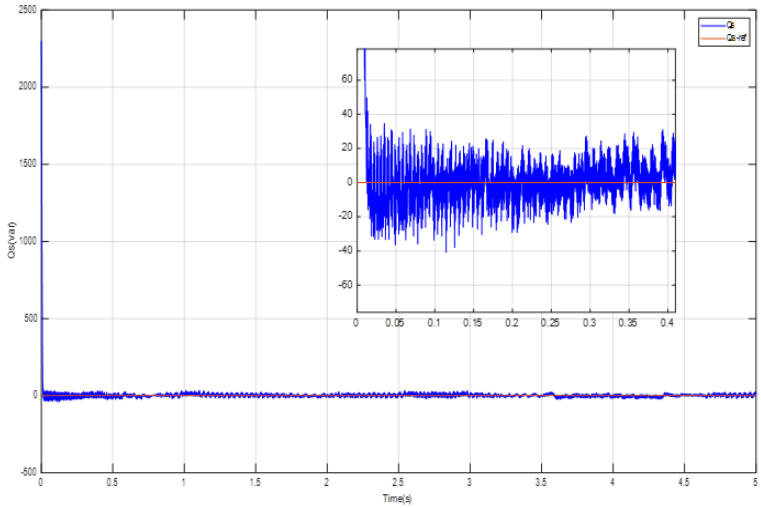

Figure 10. Reactive stator power and its reference

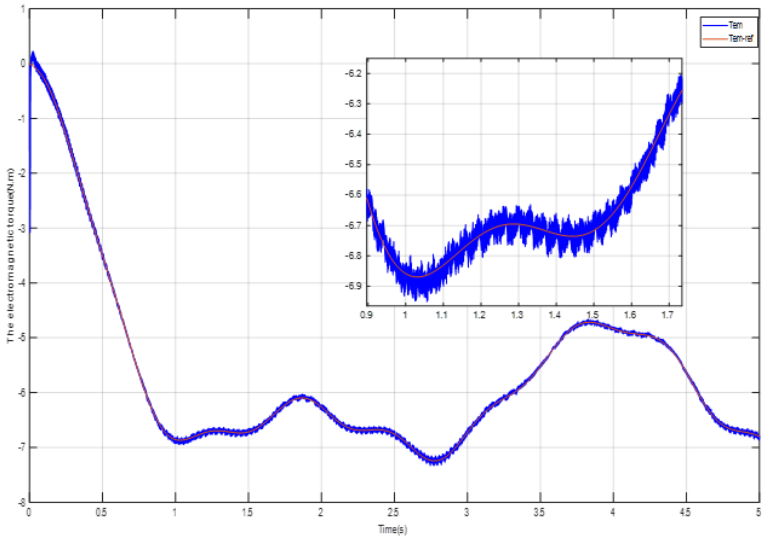

Figure 11. The electromagnetic torque and its reference

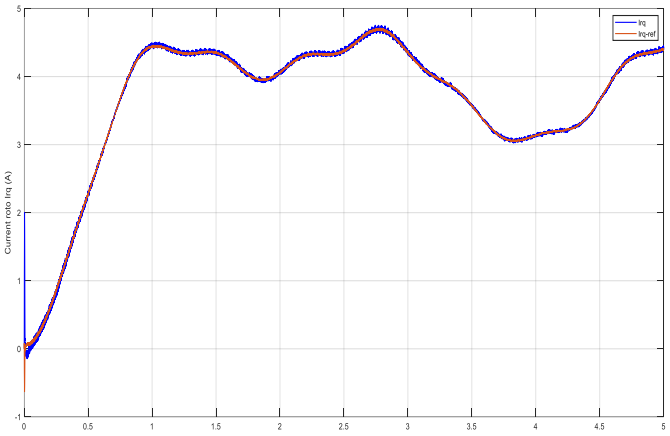

Figure 12. Current rotor I_{rq} and its reference

5.2. Backstepping control performance and robustness:

To evaluate the robustness of the proposed control command, the parameters of the generator were varied, the resistance values Rr and Rs are increased by 400% of their nominal value. Figure 13 (a) to (c) shows the variation of the reactive stator power, current rotor Irq and the torque. In these results we can observed that the fluctuations of the generator parameters have kept the same performance in terms of precision and tracking of the setpoint. It can therefore be seen that the backstepping control is robust against changes in the parameters of the DFIG.

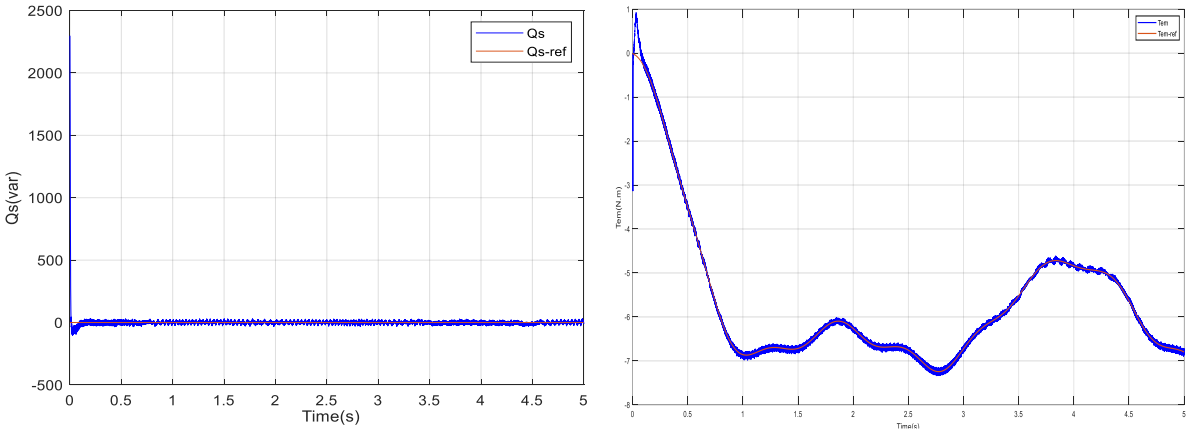

(a) (b)

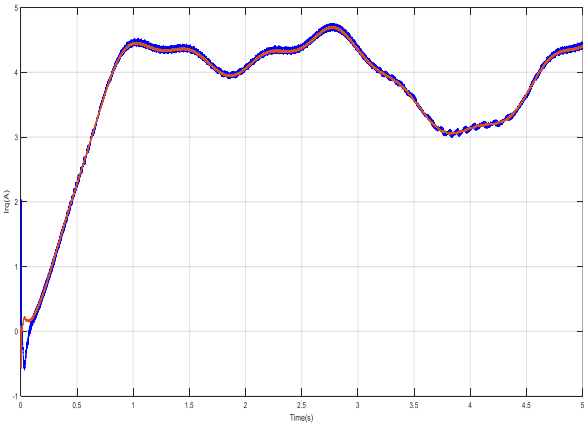

(c)

Figure 13. Robustness test (a) reactive stator power, (b) the electromagnetic torque, and (c) current rotor I_{rq}

To demonstrate the advantages and validity of the proposed control, it is beneficial to compare it with other techniques found in the literature. It should be noted that these techniques were not conducted under the same conditions, as it is quite challenging to obtain different results under identical circumstances. From Table 1, it can be observed that the proposed control-based approach exhibits a low total harmonic distortion (THD = 7.51%) compared to the other techniques. Additionally, it shows acceptable results in terms of speed and accuracy when compared to other methods in the literature, characterized by an error of 0.42% and a response time of 0.045 seconds. The parameters for the wind turbine and DFIG in this research are presented in Table 2. Figure 5 illustrates the block diagram of the backstepping control of the DFIG in this study.

Table 1. Comparison of different technical methods

Publication Paper	Control Strategy	The response time (s)	Error (%)	THD (%)
[16]	Fuzzy SMC	0.32	-	-
[17]	SMC based backstepping	0.5	-	2.98
[18]	DTC	0.2	-	18.8
[18]	FSC	0.16	-	8.26
[18]	MPDC	0.15	-	8.17
[19]	Sliding mode control	0.015	0.15	1.25
[20]	Sliding mode control for PMSG	0.1	-	-
Proposed technique	Backstepping	0.045	0.42	7.51

Table 2. Parameter of wind turbine and DFIG

Denotation	Numerical value of parameter
Rated Power	$P=1500$
Stator Resistance	$Rs=1.18$
Rotor Resistance	$Rr=1.66$
Stator Inductance	$Ls=0.20$
Rotor Inductance	$Lr=0.18$
Mutual Inductance	$M=0.17$
Frequency	$f=50$
Gain Multiplier	$G=2$
Inertia Total Moment	$J=0.04$
Radius of the Turbine	$R=1$
Optimal Tip Speed Ratio	$\lambda_{opt}=8.2$
Maximal Power Coefficient	$C_{pmax}=0.5$

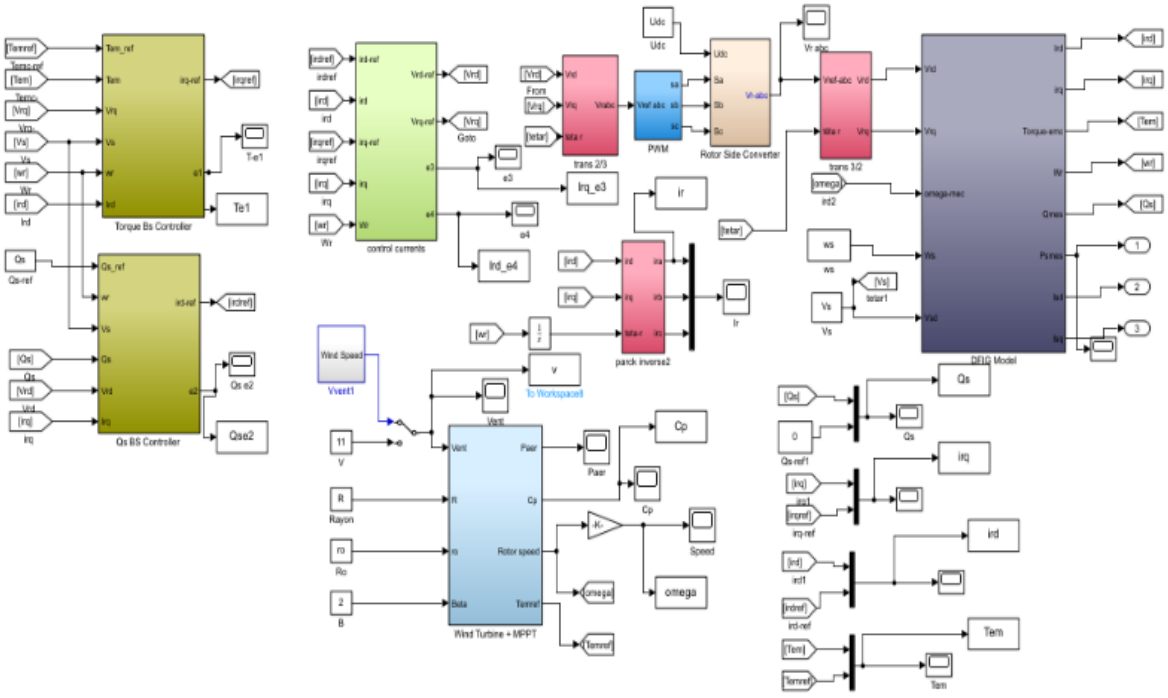

Figure 5. Diagram block of backstepping control of the DFIG

6. CONCLUSION

This paper presents a nonlinear backstepping control applied to a variable speed wind energy conversion system. After modeling the whole system (wind turbine and the double fed induction generator). We started with the MPPT control to ensure maximum power extraction. Then, we are interested by using Backstepping control in order to evaluate the system performance. For the dynamic simulation, we used MATLAB/Simulink software with a generator of nominal power of 1.5 kW, the simulation results observed clearly illustrate the performance of the Backstepping technique in terms of stability, speed and precision, as well as its robustness with respect to fluctuations in the internal parameters of the DFIG.

REFERENCES:

[1] H. Jenkal, B. Bossoufi, A. Boulezhar, A. Lilane, and S. Hariss, "Vector control of a doubly fed induction generator wind turbine," *Materials Today: Proceedings*, vol. 30, pp. 976–980, 2019, doi: 10.1016/j.matpr.2020.04.360.

[2] E. Chetouani, Y. Errami, A. Obbadi, and S. Sahnoun, "Hybrid control using adaptive particle swarm optimization and integral backstepping control of grid-connected doubly fed induction generator," *Trends in Sciences*, vol. 18, no. 23, 2021, doi: 10.48048/tis.2021.712.

[3] F. Poitiers, "Etude et commande de génératrices asynchrones pour l'utilisation de l'énergie éolienne masàca et mada," Thèse de Doctorat de l'université de NANTE, 2006.

[4] J. A. Baroudi, V. Dinavahi, and A. M. Knight, "A review of power converter topologies for wind generators," *Renewable Energy*, vol. 32, no. 14, pp. 2369–2385, 2007, doi: 10.1016/j.renene.2006.12.002.

[5] O. Anaya-Lara, N. Jenkins, J. B. Ekanayake, P. Cartwright, and M. Hughes, *Wind energy generation: modelling and control*. John Wiley and Sons, 2011. [Online]. Available: https://www.dawsonera.com/readonline/9780470748237

[6] Y. Errami, A. Obbadi, and S. Sahnoun, "Control of PMSG wind electrical system in network context and during the MPP tracking process," *International Journal of Systems, Control and Communications*, vol. 11, no. 2, pp. 200–225, 2020, doi: 10.1504/IJSCC.2020.106578.

[7] A. Boualouch, A. Essadki, T. Nasser, A. Boukhriss, and A. Frigui, "Power control of DFIG in WECS using backstipping and sliding mode controller," vol. 2, no. 6, pp. 612–618, 2015.

[8] H. Mahvash, S. A. Taher, M. Rahimi, and M. Shahidehpour, "Enhancement of DFIG performance at high wind speed using fractional order PI controller in pitch compensation loop," *International Journal of Electrical Power and Energy Systems*, vol. 104, pp. 259–268, 2019, doi: 10.1016/j.ijepes.2018.07.009.

[9] M. Bouderbala, B. Bossoufi, A. Lagrioui, M. Taoussi, H. A. Aroussi, and Y. Ihedrane, "Direct and indirect vector control of a doubly fed induction generator based in a wind energy conversion system," *International Journal of Electrical and Computer Engineering*, vol. 9, no. 3, pp. 1531–1540, 2019, doi: 10.11591/ijece.v9i3.pp1531-1540.

[10] M. Lamnadi, M. Trihi, B. Bossoufi, and A. Boulezhar, "Modeling and control of a doubly-fed induction generator for wind turbine-generator systems," *International Journal of Power Electronics and Drive Systems*, vol. 7, no. 3, pp. 982–995, 2016, doi: 10.11591/ijpeds.v7.i3.pp982-995.

[11] S. Mensou, A. Essadki, I. Minka, T. Nasser, and B. B. Idrissi, "Backstepping controller for a variable wind speed energy conversion system based on a DFIG," *Proceedings of 2017 International Renewable and Sustainable Energy Conference, IRSEC 2017*, 2018, doi: 10.1109/IRSEC.2017.8477586.

[12] B. Bossoufi *et al.*, "Rooted tree optimization for the backstepping power control of a doubly fed induction generator wind turbine: Dspace implementation," *IEEE Access*, vol. 9, pp. 26512–26522, 2021, doi: 10.1109/ACCESS.2021.3057123.

[13] M. Loucif, A. Mechernene, and B. Bossoufi, "Integral backstepping power control of DFIG based nonlinear modeling using voltage oriented control," *Lecture Notes in Networks and Systems*, vol. 211 LNNS, pp. 1725–1734, 2021, doi: 10.1007/978-3-030-73882-2_156.

[14] S. Mensou, A. Essadki, T. Nasser, and B. B. Idrissi, "An efficient nonlinear Backstepping controller approach of a wind power generation system based on a DFIG," *International Journal of Renewable Energy Research*, vol. 7, no. 4, pp. 1520–1528, 2017, doi: 10.20508/ijrer.v7i4.6112.g7192.

[15] I. Drhorhi *et al.*, "Adaptive backstepping controller for DFIG-based wind energy conversion system," in *Backstepping Control of Nonlinear Dynamical Systems*, (ANDC) Publisher: Academic Press, 2020, pp. 235–260, doi: 10.1016/B978-0-12-817582-8.00018-0.

[16] B. Bossoufi, M. Karim, and A. Lagrioui, "FPGA-based implementation sliding mode control and nonlinear adaptive backstepping control of a permanent magnet synchronous machine drive," *WSEAS Transactions on Systems and Control*, vol. 9, no. 1, pp. 86–100, 2014.

[17] M. Chakib, A. Essadki, and T. Nasser, "A comparative study of PI, RST and ADRC control strategies of a doubly fed induction generator based wind energy conversion system," *International Journal of Renewable Energy Research*, vol. 8, no. 2, pp. 964–973, 2018, doi: 10.20508/ijrer.v8i2.7645.g7383.

[18] X. Yang, G. Liu, V. D. Le, and C. Q. Le, "A novel model-predictive direct control for induction motor drives," *IEEJ Transactions on Electrical and Electronic Engineering*, vol. 14, no. 11, pp. 1691–1702, 2019, doi: 10.1002/tee.22992.

[19] H. El Alami *et al.*, "Fpga in the loop implementation for observer sliding mode control of dfig-generators for wind turbines," *Electronics (Switzerland)*, vol. 11, no. 1, 2022, doi: 10.3390/electronics11010116.

[20] S. E. Rhaili, A. Abbou, S. Marhraoui, R. Moutchou, and N. El Hichami, "Robust sliding mode control with five sliding surfaces of five-phase PMSG based variable speed wind energy conversion system," *International Journal of Intelligent Engineering and Systems*, vol. 13, no. 4, pp. 346–357, 2020, doi: 10.22266/IJIES2020.0831.30.

BIOGRAPHIES OF AUTHORS

Hasnaa Jenkal is a Ph.D. student in Electrical and Energy Engineering from Faculty of Sciences Ain-Chock, Casablanc Morocco. She is member of Laboratory of renewable energy and dynamic of systems (LERDYS). She had her master's degree in renewable energy and dynamic of systems at the Faculty of Sciences Ain-Chock, Casablanc Morocco. Her research interests include renewable energy (solar and wind energy), power electronics and systems modelling, static converters, MATLAB simulation, and electrical motor drives. She can be contacted at email: jenkal.hasnaa@gmail.com.

Mouna Lamnadi was born in Beni Mellal, Morocco on March 25, 1990. In 2017, she obtained a Ph.D. in Electrical Engineering and Renewable Energy from Hassan II University, Faculty of Sciences Aïn Chock-Casablanca, Morocco. She obtained the Master's degree in renewable energy and energy systems from the same university in 2013. Her research interests include static converters, electric motor drives, power electronics, smart grids and hybrid renewable energy systems (HRES).

Sara Mensou is a Doctor of Engineering at Ecole Nationale Supérieure d'Arts et Métiers Rabat. She is a member of Electrical Engineering Department of ENSET, Mohammed V University, BP 6207 Rabat, Morocco. Her research expertise includes MATLAB simulation, electrical power engineering, renewable energy technologies, power electronics and power systems modelling.

Badre Bossoufi is a Professor of Electrical Engineering, at Faculty of Sciences, Sidi Mohamed Ben Abdellah University, Fez Morocco. He is member of laboratory (LIMAS). He received the Ph.D. degree in Electrical Engineering from University Sidi Mohammed Ben Abdellah, Faculty of Sciences, Morocco and Ph.D. degree from University of Pitesti, Faculty of Electronics and Computer, Romanie and Montefiore Institute of electrical engineering, Luik, Belgium. His research interests include static converters, electrical motor drives, power electronics, smart grid, renewable energy and artificial intelligent.

Abdelkader Boulezhar is a Professor of Molecular Spectroscopy and Dosimetry at Faculty of sciences Ain Chock, Physics, Hassan II University-Casablanca Morocco. He is Head of Physics Department and member of Laboratory renewable energy and dynamic of systems (LERDYS). His research interests include renewable energy, material sciences, plasma, molecular spectroscopy and optics